Phase diagrams of site-frustrated Heisenberg models on simple cubic, bcc, and fcc lattices

A. D. Beath and D. H. Ryan
Physics Department and Centre for the Physics of Materials, McGill University, 3600 University Street, Montreal, Quebec, Canada, H3A 2T8

(Received 15 March 2006; revised manuscript received 17 May 2006; published 29 June 2006)

We have determined the phase diagrams of the site-frustrated Heisenberg model in three dimensions over the entire concentration regime of competing ferromagnetic (F) and antiferromagnetic (A) sites for the three basic lattice types: simple cubic (sc), body-centered cubic (bcc) and face-centered cubic (fcc) using Monte Carlo methods. Long-range ferromagnetic (FM) or antiferromagnetic (AF) order is established at a finite temperature, second-order phase transition whenever F or A sites percolate. Since site percolation thresholds in three dimensions are less than $\frac{1}{2}$, FM and AF order coexist over a wide composition regime. The only apparent effect of frustration is to cause the AF and FM order to occur perpendicular to one another. Strong evidence is found to suggest that all of the transitions remain in the Heisenberg universality class and that there exists a tetracritical point at $x=\frac{1}{2}$ where $T_C=T_N$.

DOI: 10.1103/PhysRevB.73.214445 PACS number(s): 75.50.Lk, 02.70.Uu, 75.10.Hk, 75.40.Mg

I. INTRODUCTION

Some of the most studied spin-glass materials are made by mixing ferromagnetic (F) and antiferromagnetic (A) sites together in an amorphous solid, a typical example being[1–3] amorphous a-$(Fe_{1-x}Mn_x)$G, where G is a glass former, such as Si. The concentration-temperature (x-T) phase diagram of this material is shown in Fig. 1. The main features are (i) on increasing x from zero, the Curie temperature T_C steadily decreases; (ii) above a critical concentration $x_{c_1}\sim 0.17$, a second transition develops at T_{xy} below T_C where spin-glass order coexists transverse to the established FM order; (iii) above $x_{c_2}\sim 0.32$ FM order disappears and the material exists as a spin glass. A minimal model, which is thought to capture the essential physics of these types of materials, is the site-frustrated Heisenberg model, where F and A sites are distributed at random on a lattice.

The first to study this model, to the best of our knowledge, was Aharony[4] who used renormalization group techniques. His phase diagram, for bipartite lattices, is similar to ours [see Figs. 2(a) and 2(b)], in that a tetracritical point bounds a mixed phase consisting of coexisting FM and AF order. Further work,[5] however, cast doubt on his original result, although it is important to note that a true site-frustrated model was not being considered in this later work. Instead, a site-frustrated model was considered to be equivalent to a bond-frustrated model[6] where, rather than a random distribution of F and A sites, one considers a random mixture of F and A bonds; the well-known Edwards-Anderson spin-glass model.[7] Within mean field theory, the phase diagram of the bond-frustrated model is well understood[8] and is thought to capture the physics of a different class of materials, such as Refs. 1 and 9 a-$Fe_{1-x}Zr_x$. However, as we shall prove, the site-frustrated model is not equivalent to a bond-frustrated model and the phase diagrams are fundamentally different.

The best results for the site-frustrated Heisenberg model have been obtained from Monte Carlo simulations,[10–13] yet the authors disagree in their interpretations of the phase diagram. Two studies[10,12] claim that a mixed noncollinear phase, similar to spin-glass order, exists in the vicinity of $x=\frac{1}{2}$. On the other hand, we[13] and others[11] have claimed that the mixed phase consists of coexisting FM and AF order, and that the AF- and FM-ordering vectors are mutually perpendicular. In addition, it has been reported[11,12] that the ferromagnetic transition belongs to the Heisenberg universality class for small x, and that with increasing x the universality class of the transition changes, in contradiction to the Harris criterion.[14] Bekhechi and Southern[12] have also claimed that the tetracritical point, where $T_C(x)=T_N(x)$, does not exist and instead there exists a regime $0.52<x<0.48$ where $T_C(x)=T_N(x)$. Resolving the different interpretations is important since one would like to identify the minimal physics necessary to understand the phase diagrams of real materials.

Here we present the results of extensive Monte Carlo simulations on three different lattice types: sc, bcc, and fcc.

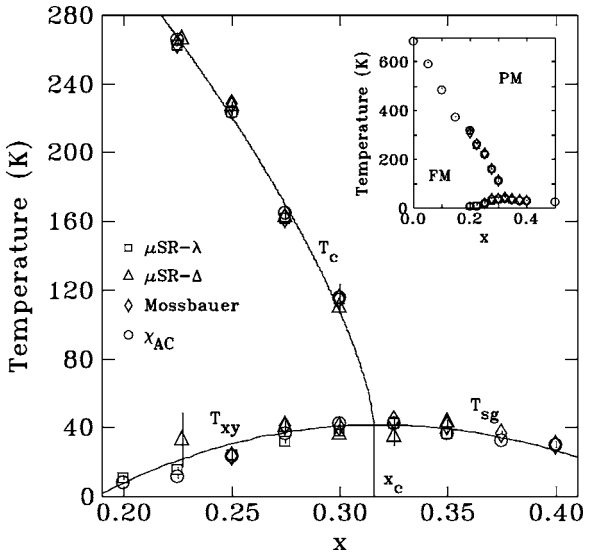

FIG. 1. Phase diagram for a-$(Fe_{1-x}Mn_x)_{78}Si_8B_{14}$ obtained from μSR, Mössbauer spectroscopy, and magnetometry. T_C marks the line separating paramagnetic and ferromagnetic phases. T_{XY} marks the onset of transverse spin freezing, occurring for $0.17<x<0.32$. T_{SG} marks the onset of spin-glass order, occurring for $x>0.32$. For details see Ref. 2.

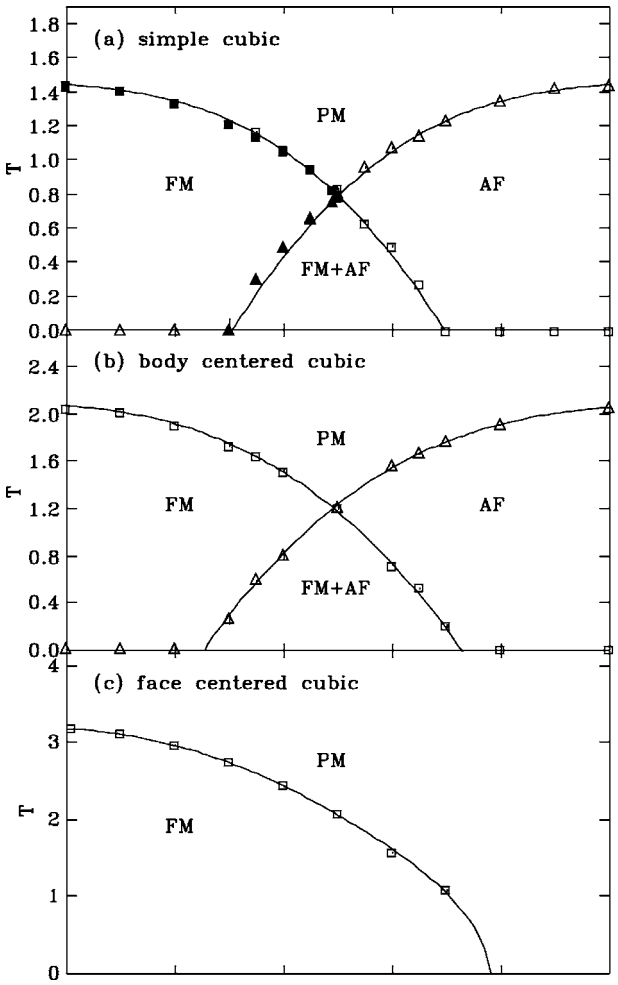

FIG. 2. Phase diagrams of the site-frustrated Heisenberg model for (a) simple cubic (b) bond-centered-cubic and (c) face-centered-cubic lattices. Transitions marked by solid symbols in (a) are obtained with 200+ configurations of disorder, and system sizes $L=4,6,8,10,12,16,20$, and 24. Transition temperatures and errors are given in Table II. Transitions marked by open symbols are obtained from 16+ configurations only, and smaller system sizes. Lines marking phase boundaries are guides to the eye.

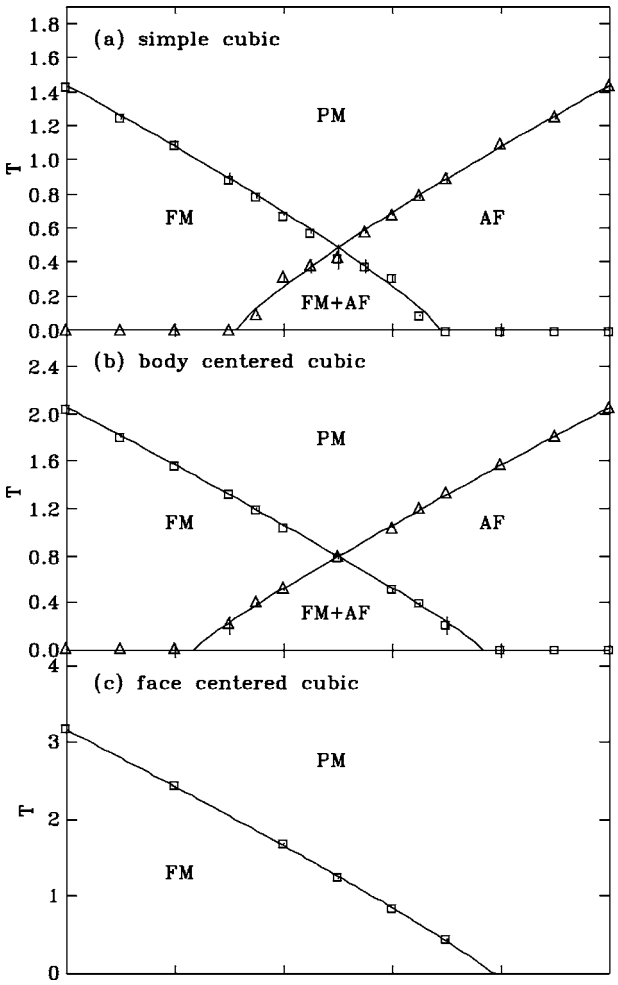

FIG. 3. Phase diagrams of the nonfrustrated model with $J_{FA}=0$ for (a) simple cubic, (b) bond-centered-cubic, and (c) face-centered-cubic lattices. The phase diagrams are, aside from a rescaling of the transition temperatures, identical to those of the site-frustrated Heisenberg model shown in Fig. 2. Lines marking phase boundaries are guides to the eye.

Our phase diagrams, shown in Fig. 2 for simple-cubic (sc), body-centered-cubic (bcc) and face-centered-cubic (fcc) lattices, are somewhat different from the phase diagrams given in all previous Monte Carlo studies.[10–12] If F and A sites do not interact, the model can be readily understood from the theory of dilute magnetism:[15] When a percolating cluster of F(A) sites forms, a finite temperature transition is found at $T_C(T_N)$ and the transitions remain in the Heisenberg universality class. For bipartite lattices with symmetric interactions, a *decoupled* tetracritical point is found at $x=0.5$, since by symmetry $T_C(x)=T_N(x)$. The tetracritical point is referred to as "decoupled" since the simultaneous FM- and AF-ordering events have no impact on each other if the exchange interaction between F and A sites is zero. The phase diagrams for this model, with no interaction between F and A sites, is shown in Fig. 3 for sc, bcc, and fcc lattices. Introducing an interaction between F and A sites yields the site-frustrated Heisenberg model. We find that the ordering is essentially as one would expect if F and A sites did not interact, and as such there exists a tetracritical point at $x=0.5$, and the transitions remain in the Heisenberg universality class. The only notable effects introduced by coupling the AF and FM order together are a rescaling of the transition temperatures and perpendicular FM- and AF-ordering vectors.

As the loss of order in the nonfrustrated model is associated with site percolation, and percolation thresholds are determined by the lattice coordination, we have extended our study of the site-frustrated model to include bcc and fcc lattices. Here we show that the same site percolation mechanism likely controls the loss of order in site-frustrated models as well.

Within our picture, the site-frustrated Heisenberg model on bipartite lattices cannot account for the phase diagrams of materials like a-$(Fe_{1-x}Mn_x)$G since a spin-glass phase is not realized at any composition. The lack of a spin-glass phase is due to insufficient frustration in the bipartite lattices. Increasing the concentration of frustration can be accomplished by considering a nonbipartite lattice, such as fcc. The site-

frustrated Heisenberg model on an fcc lattice, which is geometrically frustrated with respect to AF order (as are amorphous solids), is therefore more likely to capture the ordering of glassy materials.

II. MODELS, SYMMETRIES, AND METHODS

A. Site-frustrated Heisenberg model

The site-frustrated model we consider here is a classical Heisenberg model with the Hamiltonian

$$\mathcal{H} = -\sum_{\langle ij \rangle} J_{ij} \vec{S}_i \cdot \vec{S}_j, \tag{1}$$

where the sum runs over all nearest-neighbor bonds J_{ij}. The distribution of bonds in site-frustrated models can be expressed as

$$J_{ij} = J_{FF} x_i x_j + J_{AA}(1-x_i)(1-x_j) + J_{FA}[x_i(1-x_j) + x_j(1-x_i)], \tag{2}$$

where $x_i=1$ if site i is occupied by a F (ferromagnetic) site and $x_i=0$ if site i is occupied by an A (antiferromagnetic) site. For random F/A occupancy, the probability of site i being F type $P(x_i=1)=(1-x)$ and the probability of site i being A type $P(x_i=0)=x$. Our site-frustrated model corresponds to the choice

$$J_{FF} = -J_{AA} = -J_{FA} = 1. \tag{3}$$

We have chosen $J_{FA}=-1$ since in our experimental work[2,3] on a-$(Fe_{1-x}Mn_x)$G, bulk magnetization, Mössbauer spectroscopy, and μSR measurements all show that for small x, the Mn moments orient opposite to the Fe-rich FM bulk. However, the phase diagram is invariant with respect to the sign of J_{FA} for bipartite lattices, and thus, this choice of sign is unimportant. We have considered three different lattice types, sc, bcc, and fcc with linear dimension L containing $N=L^3$, $N=2L^3$, and $N=4L^3$ sites, respectively, with periodic boundary conditions and L even. The phase diagrams for sc, bcc, and fcc lattices are shown in Fig. 2.

We have also considered a related (and trivial) nonfrustrated model with

$$J_{FF} = -J_{FA} = 1 \quad \text{and} \quad J_{FA} = 0. \tag{4}$$

The phase diagrams for this model are shown in Fig. 3 for sc, bcc, and fcc lattices. As mentioned in the Introduction, when F and A sites do not interact ($J_{FA}=0$), we expect finite $T_C(T_N)$ provided only that F(A) sites percolate. Since for sc lattices the percolation threshold is $x_p=0.312$,[16] one expects this model to have a mixed phase of coexisting FM and AF order for $0.312<x<0.688$, as is observed. For bcc lattices,[16] $x_p=0.245$ and a mixed phase is expected for $0.245<x<0.755$, also observed. For the fcc lattice,[16] where $x_p=0.198$ we observe a FM phase for $0\le x<0.802$. For the fcc lattice, we have not measured the AF order, which is more complex than in the bipartite lattices, and thus, we have not observed a mixed phase. Note that, aside from a minor rescaling of the transition temperatures, the phase diagrams of site-frustrated models (Fig. 2) are identical to those of nonfrustrated models (Fig. 3).

It is important to note that we do not consider the choice $J_{FF}=J_{AA}=-J_{FA}=1$, a Mattis model,[17] which has no frustration. The site-frustrated model we consider here is, however, equivalent to Luttinger's site-frustrated model[18] (with $J_1=-J_2=J_3=\frac{1}{2}$) which, for Ising spins, exhibits spin-glass ordering in the mean field limit.

B. Gauge invariance and symmetries

In the presence of a random distribution of bimodal interactions, $(J_{ij}=\pm 1)$, a Hamiltonian of the type shown in Eq. (1) will possess a number of useful symmetries. Frustration is the property that, given a set of spins $\{\vec{S}_i\}$ linked with a closed loop of nonzero J_{ij}, no set $\{\vec{S}_i\}$ exists that can satisfy all of the interactions J_{ij}. Frustration is measured by considering the value of the frustration function[19,20]

$$\phi = \prod J_{ij} \tag{5}$$

evaluated around a plaquette—the smallest closed loop of S_i linked by nonzero J_{ij}. If $\phi<0$, then a plaquette is frustrated, whereas if $\phi>0$, the plaquette is not frustrated. Since Eq. (5) always contains even powers of J_{FA} for a site-frustrated model, frustration is independent of the sign of J_{FA}. It follows that frustration is only present if $J_{FF}=-J_{AA}$.

Model symmetries can be found by considering a local transformation of the spin and bond variables according to[20]

$$\vec{S}_i \to -\vec{S}_i, \quad J_{ij} \to -J_{ij}, \tag{6}$$

where a spin at site i is inverted as well as all of the bonds J_{ij} emanating from site i. Any set of such local transformations

$$G(\{\tau_i\})[\{\vec{S}_i\};\{J_{ij}\}] = [\{\tau_i \vec{S}_i\};\{\tau_i J_{ij} \tau_j\}] \tag{7}$$

with $\tau_i=\pm 1$, called a gauge transformation, preserves both the Hamiltonian and the distribution of frustration.[20] Since the Hamiltonian is invariant under any $G(\{\tau_i\})$, the partition function and the free energy are also invariant. It follows that any pair of models with different distributions of the variables J_{ij}, yet having the same distribution of frustration, have the same phase diagram (the order parameters are, in general, different).

A first symmetry is revealed using the gauge transformation

$$G(\tau_A = \pm 1; \tau_F = \mp 1), \tag{8}$$

which inverts the spins of either all A or all F sites in the lattice. The bonds are transformed such that $J_{FA} \to -J_{FA}$ while both J_{FF} and J_{AA} remain invariant. Therefore, phase diagrams of site-frustrated models (provided $|J_{FF}|=|J_{AA}|$) are invariant with respect to the sign of J_{FA}.

A second symmetry occurs for bipartite lattices that can be decomposed into two interpenetrating sublattices α and β. The gauge transformation

$$G(\tau_\alpha = \pm 1; \tau_\beta = \mp 1) \tag{9}$$

has the effect of flipping the sign of all of the bonds so that $J_{ij} \to -J_{ij}$. This is equivalent to taking a model with a concentration x of A sites $(1-x$ of F sites) and creating a model

with a concentration $1-x$ of A sites (x of F sites), while also flipping J_{FA}, which, as we have already shown, is irrelevant. Therefore, for bipartite lattices, the phase diagrams must be symmetrical about $x=\frac{1}{2}$.

The symmetry between ferromagnetic and antiferromagnetic models on bipartite lattices found by using the gauge transformation given by Eq. (9) only applies to lattices with L even. If L is odd, as in the simulations of Matsubara *et al.*,[11] then two equivalent sublattices do not exist, and for this reason we believe these results should be considered with caution.

One effect of Eq. (9) is to transform the FM-order parameter m_f into the AF-order parameter m_{st}, and vice versa. Thus, if the model orders as a collinear FM, a collinear AF, or a mixture of the two (whose order need not be parallel), then gauge symmetry implies the following symmetry between the order parameters m_f and m_{st}:

$$m_f(x,T;J_{FA}) = m_{st}(1-x,T;-J_{FA}) \tag{10}$$

$$m_{st}(x,T;J_{FA}) = m_f(1-x,T;-J_{FA}) \tag{11}$$

for all x and T. This symmetry also applies to all higher-order powers of m_f and m_{st}, and therefore the susceptibilities are also symmetric under the exchange $x\rightarrow(1-x)$, $J_{FA}\rightarrow -J_{FA}$. This symmetry persists even when the ordering does *not* consist of a mixture of collinear FM and AF order, as, for example, spin-glass order. However, in the case of spin-glass order, m_f and m_{st} would scale to zero in the limit of large L. The fact that we observe a nonzero m_f and/or m_{st} in the limit of large L for bipartite lattices excludes any possibility that the mixed phase is a spin-glass phase.

C. Monte Carlo methods

Our study of the site-frustrated Heisenberg model has proceeded in two parts. In the first, we have employed a simple Metropolis Monte Carlo algorithm with simulated annealing to obtain the phase diagrams shown in Figs. 2 and 3. The system sizes studied range from $4\leq L\leq 16$ (sc), from $4\leq L\leq 14$ (bcc), and from $4\leq L\leq 12$ (fcc) for the concentrations shown in the phase diagrams by open symbols. The range of system sizes for sc lattices are the same as those used in Refs. 11 and 12. For the sc and bcc lattices with $J_{FA}=0$ [Figs. 3(a) and 3(b)], only $x\leq 0.5$ were studied and $T_{C,N}(x>0.5)$ are obtained by symmetry. The number of Monte Carlo updates per lattice site (MCS) ranged from 5×10^3 to 5×10^6 after discarding the first 5×10^3 to 5×10^4 MCS at each T to ensure equilibration. The number of MCS is chosen such that we exceed the measured sample independence time, given by twice the integrated autocorrelation time[21,22] τ, by orders of magnitude. The large value of τ, which occurs near and below $T_{C,N}$, limits the lattice sizes and the number of disorder configurations studied. In this initial survey, a minimum of 16 realizations of disorder were used to obtain configurational averages.

In order to increase L, and the number of configurations C, we must reduce τ. To do so, we have employed an overrelaxation scheme,[23] where the spins evolve according to

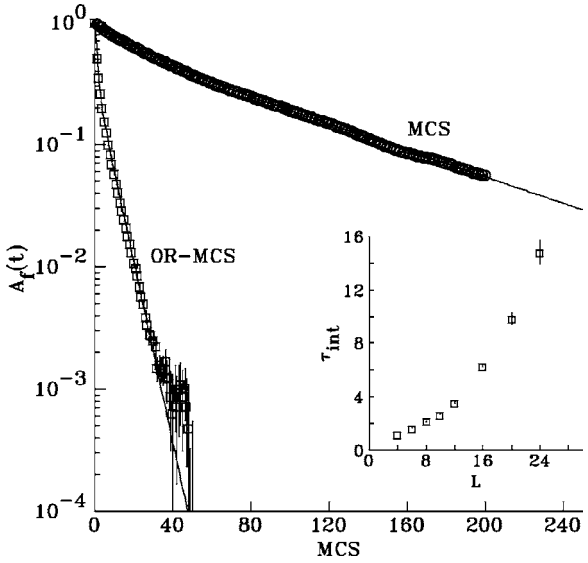

FIG. 4. Autocorrelation function for the magnetisation [Eq. (13)] using Metropolis (MCS) and Metropolis plus over-relaxation (OR-MCS) dynamics for $T\sim T_C$ ($L=10, x=0.45$). The inset shows the integrated integrated autocorrelation time at $T=0.95$ using over-relaxation plus Metroplolis dynamics.

$$\vec{S}_i \rightarrow 2\frac{\vec{S}_i\cdot\vec{B}_i}{\vec{B}_i\cdot\vec{B}_i}\vec{B}_i - \vec{S}_i, \tag{12}$$

where $\vec{B}_i=\Sigma_j J_{ij}\vec{S}_j$ is the internal field experienced at site i due to the coupling with nearest-neighbor spins $\vec{S}_j$. Following each Metropolis MCS we use five overrelaxation MCSs, which then comprises a single OR-MCS. The OR-MCS update has reduced τ by about a factor of 100. However, there remains a divergence of τ according to $\tau\sim L^z$ with z unaltered from the value found using only Metropolis dynamics ($z\sim 0$, $z\sim 2$, and $z\sim 3$ for $T\gg T_C$, $T\sim T_C$ and $T\ll T_C$, respectively). Overrelaxation has been found useful in studies of the site-frustrated Heisenberg model,[11] the bond-frustrated Heisenberg model,[24] and fcc Heisenberg antiferromagnets.[25]

The dramatic reduction in τ that occurs when employing the overrelaxation update is illustrated in Fig. 4, where we have plotted the normalized autocorrelation function of the magnetization near T_C for MCS and OR-MCS updates. The autocorrelation function of the magnetization or staggered magnetization [$A_f(t)$ and $A_{st}(t)$, respectively] at time t is given by

$$A_{f,st}(t) = [\langle m_{f,st}(0)m_{f,st}(t)\rangle] - [\langle m_{f,st}\rangle]^2, \tag{13}$$

where the angular brackets represent a time average and the square brackets represent a configurational average (m_f and m_{st} are defined below). The decays $A_{f,st}(t)$ are comprised of a discrete sum of exponential decays,[22] and the derived autocorrelation time is shown in the inset of Fig. 4 for $T\sim T_C$ using the OR-MCS update.

The OR-MCS update has enabled us to equilibrate larger sc lattices with $4\leq L\leq 24$. The number of configurations used at each x and L is listed in Table I. The number of OR-MCS used here ranges from 5×10^2 at high temperatures

TABLE I. Number of disorder configurations (C) used for each concentration (x) and system size (L) for sc lattices using the OR-MCS Monte Carlo update as explained in the text.

L	x=0.10	0.20	0.30	0.35	0.40	0.45	0.49	0.50
4	200	200	200	200	200	1600	1600	1600
6	200	200	200	200	200	872	592	962
8	200	200	200	200	200	976	800	560
10	200	200	200	200	200	976	403	520
12	200	200	200	200	200	744	208	728
16	200	200	200	200	200	400	240	299
20	200	200	200	200	200	400	240	286
24	256	244	224	184	208	288	234	240

to 5×10^4 at low temperatures, after discarding between 5×10^2 to 5×10^3 OR-MCS to ensure equilibration. Again, the number of OR-MCS is chosen to be much larger than any measurable sample independence time. The resulting phase diagram is shown in Fig. 2(a) by solid symbols, and summarized in Table II. These results are more accurate than our original survey, although the form of the phase diagram remains unaltered.

Two characteristics of the $A_{f,st}(t)$ decays have been extensively checked to ensure that our results are both equilibrated and representative of the limit $t\to\infty$. Equilibrium requires that the $A_{f,st}(t)$ decays are independent of the origin of time. For selected concentrations and temperatures, we have verified that the decays are repeatable, and thus equilibrated, by measuring $A_{f,st}(t)$ while varying the number of discarded MCSs (or OR-MCSs) prior to the measurement. Indeed, accurate measurement of $A_{f,st}(t)$ requires that the number of MCSs exceeds τ by orders of magnitude, which essentially guarantees this result. To ensure our results are equilibrated at each temperature, we discard several τ's worth of MCSs (or OR-MCSs) prior to our measurements.

To check that our results are representative of the long time limit, we have compared our results when varying the numbers of MCS or OR-MCS updates. The $A_{f,st}(t)$ decays provide a measure of τ for the *scalar* quantity $m_{f,st}$, while our demonstration, presented later, that the FM and AF order are mutually perpendicular, required us to exceed τ for the *vector* quantities $\vec{m}_{f,st}$. Since τ for vector order parameters is much larger than for scalar order parameters, the long times necessary to demonstrate that the FM order and AF order are perpendicular also allows us to compare $m_{f,st}$ measured in typical simulations (with $\sim5\times10^4$ MCSs) to that measured in a very long and atypical simulation (with $\sim5\times10^6$ MCSs). The comparison confirms that exceeding τ by orders of magnitude yields results that are characteristic of the limit $t\to\infty$.

TABLE II. Critical temperatures for the site-frustrated Heisenberg model for the sc lattice type. Note that by symmetry $T_C(x)=T_N(1-x)$.

x	$T_C(x)$	$T_N(x)$
0.10	1.4155(6)	
0.20	1.3389(9)	
0.30	1.2189(7)	
0.35	1.1420(17)	0.2980(22)
0.40	1.0546(8)	0.4862(23)
0.45	0.9491(6)	0.6576(25)
0.49	0.8259(18)	0.7536(32)
0.50	0.7804(13)	0.7794(4)

The most important quantities we measure are powers of the finite lattice magnetization and staggered magnetization. At time t, the instantaneous values of the nth power of the magnetization or staggered magnetization, m_f and m_{st}, are

$$m_{f,st}^n=\left[\left(N^{-1}\sum_i L_{f,st}^i S_i^x\right)^2+\left(N^{-1}\sum_i L_{f,st}^i S_i^y\right)^2+\left(N^{-1}\sum_i L_{f,st}^i S_i^z\right)^2\right]^{n/2},\tag{14}$$

where x,y,z denote Cartesian components and $L_{f,st}^i$ is an operator with the symmetry of the ferromagnetic or antiferromagnetic state. We have not made an attempt to measure the AF order for the fcc lattice, which is more complex than the AF order in bipartite lattices.[25] Average values are obtained by averaging over time (angular brackets) and disorder (square brackets) to yield $[\langle m_f^n\rangle]$ and $[\langle m_{st}^n\rangle]$. For brevity, we will henceforth refer to $[\langle m_{f,st}\rangle]$ as $m_{f,st}$ with the understanding that averages over time and disorder have been taken. Other quantities of interest are the connected ferromagnetic and antiferromagnetic susceptibilities, χ_f^c and χ_{st}^c, given by

$$\chi_{f,st}^c=N\beta[\langle m_{f,st}^2\rangle-\langle m_{f,st}\rangle^2]\tag{15}$$

and the disconnected ferromagnetic and antiferromagnetic susceptibilities, χ_f^d and χ_{st}^d, given by

$$\chi_{f,st}^d=N\beta[\langle m_{f,st}^2\rangle]\tag{16}$$

Lastly, we have measured the Binder cumulant for the ferromagnetic and antiferromagnetic state, $B_{f,st}$, given by

$$B_{f,st}=\frac{1}{2}\left(5-3\frac{[\langle m_{f,st}^4\rangle]}{[\langle m_{f,st}^2\rangle]^2}\right),\tag{17}$$

which is helpful in locating T_C and T_N. The normalization is chosen such that $B_{f,st}=0$ at $T=\infty$ and, in the case of the pure $(x=0,1)$ models, $B_{f,st}=1$ at $T=0$.

III. RESULTS

The phase diagrams we have found for $J_{FA}=-1$ (Fig. 2) and $J_{FA}=0$ (Fig. 3) bear a striking similarity: FM order occurs provided F sites percolate and AF order occurs (for sc and bcc lattices) provided A sites percolate. At low temperatures within the mixed phase, m_f and m_{st} account for the majority of the total spin (at $x=0.5$ $m_f+m_{st}\sim0.8$). Furthermore, bipartite lattices always show either ferromagnetic order, antiferromagnetic order, or a mixture of the two, and thus, the possibility of a spin-glass phase—which lacks any periodic order—can be conclusively ruled out.

The important difference between our phase diagram on the sc lattice and the phase diagrams found by others[10–12]

are: (i) Both Matsubara *et al.*[11] and Bekhechi *et al.*[12] have claimed that for large enough x, $T_C(x)$, and by symmetry $T_N(1-x)$, do not remain in the Heisenberg universality class and (ii) the existence of a tetracritical point has been challenged;[12] instead they suggest that there is a range of concentrations for which $T_C(x)=T_N(x)$. Our results are at odds with both since we find (i) that all transitions remain in the Heisenberg universality class and (ii) there is no evidence to support the existence of a range of concentrations for which $T_C(x)=T_N(x)$. Instead, we conclude that the model, for bipartite lattices, possess a tetracritical point. The differences are related, we believe, to a misidentification of the transition temperatures.

In all cases where Bekhechi and Southern[12] claim that the model remains in the Heisenberg universality class, our estimates of $T_{C,N}$ are in agreement with theirs. By constrast, in all cases where they claim the model does *not* remain in the Heisenberg universality class, our estimates of $T_{C,N}$ are *not* in agreement.

To determine the form of the phase diagram, we have extracted the system-size dependent pseudotransition temperatures $T_{C,N}(L)$ from the peak in $\chi^c_{f,st}$ and the maximum slope in $B_{f,st}$. According to finite size scaling theory, we expect that $T_{C,N}(L)$ should, for large enough L, scale according to

$$T_{C,N}(L) = T_{C,N} + aL^{-1/\nu}, \tag{18}$$

where ν is the exponent of the correlation length. Equation (18) allows us to locate T_C and T_N. We begin by assuming that the model remains in the Heisenberg universality class, for which the exponent ν takes the value $\nu=0.704$.[26,27] Scaling plots for several concentrations are shown for the sc lattice in Fig. 5 for both T_C and T_N. With increasing L, the data begin to fall onto straight lines [see also Fig. 9(b)], indicating that corrections to scaling are important for the smaller lattices. For $L>8$ ($\chi^c_{f,st}$) and $L>10$ ($B_{f,st}$), the $T_{C,N}(L)$ are linear in $L^{-1/\nu}$ and yield the same estimates for T_C and T_N within error. In the case of the pure model ($x=0$), the asymptotic scaling regime beyond which corrections to scaling become negligible is also[27] $L\sim 10$, and so the deviations at small L are to be expected. Straight-line fits for $L>10$ yield two independent estimates for both T_C and T_N, and the weighted average of the two estimates are summarized in Table II for $x\leq 0.5$. Although the estimates for T_C and T_N so obtained are our most precise results, they do depend on the assumption of universality. However, estimates found assuming universality are consistent with other estimates, in particular, those found from crossings of the Binder cumulant, which make *no* reference to a particular universality class.

The analysis that led to the phase diagram shown in Fig. 2(a) assumed that the site-frustrated Heisenberg model remains in the three-dimensional Heisenberg universality class. That the transition temperatures found assuming this universality are correct is demonstrated in Fig. 6, where we have plotted the crossing of the Binder cumulant B_f for $x=0.45$. According to finite size scaling theory, $B_{f,st}$ should scale as

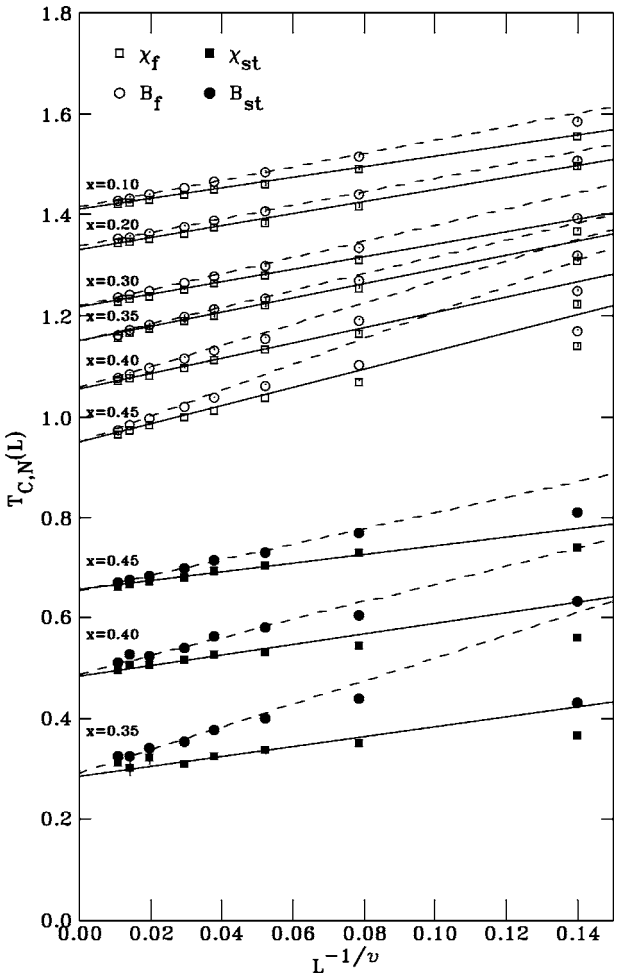

FIG. 5. Finite size scaling of the pseudotransition temperatures $T_C(L)$ and $T_N(L)$ for the site-frustrated Heisenberg model on sc lattices. Lattice sizes $L=4,6,8,10,12,16,20$, and 24. The exponent $\nu=0.704$ is taken for the Heisenberg universality class. Solid lines are fits, for $L>8$, to $T_{C,N}(L)$ [Eq. (18)], obtained from the peak in χ^c. Dashed lines are fits, for $L>10$, to $T_{C,N}(L)$ obtained from the maximum slope in $B_{f,st}$. Where error bars are not apparent, they are smaller than the symbol size.

$$B_{f,st} = B_{f,st}(tL^{1/\nu}), \tag{19}$$

where $t=(T-T_{C,N})/T_{C,N}$ is the reduced temperature. Thus, a plot of $B_{f,st}$ for different L should exhibit a crossing at $T_{C,N}$. Note that the location of this crossing is independent of the universality class of the transition. The crossing near $T_C=0.947(5)$ is clear and agrees well with our estimate $T_C=0.9491(6)$ found from Fig. 5, where we assumed that the model was in the Heisenberg universality class in order to extract T_C. Our value is both far from the earlier estimate[12] $T_C=0.925(5)$, and more precise. At $x=0.45$, they estimated that $\nu\sim 1$.[12] However, as shown in the inset of Fig. 6, the Binder parameter scales very well using Eq. (19) with $\nu=0.704$ provided $L>8$.

More evidence to support our conjecture that the model remains within the Heisenberg universality class is found in the scaling of the order parameters and their fluctuations.

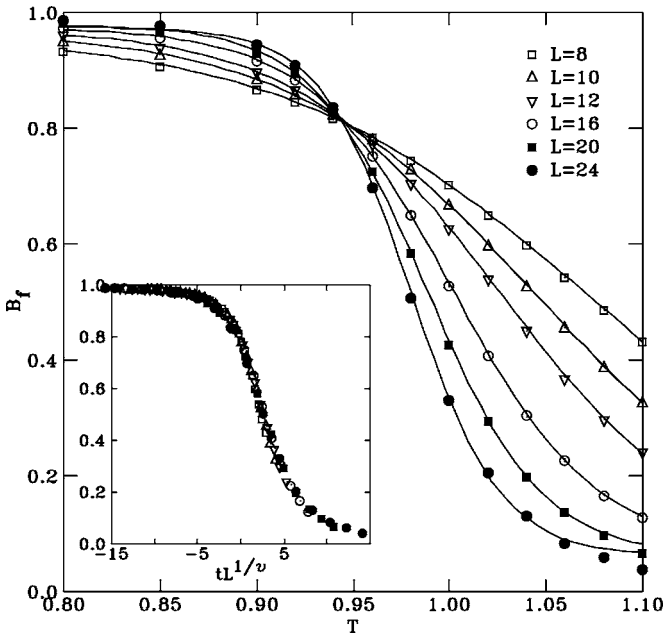

FIG. 6. Binder cumulant B_f of the ferromagnetic order near T_C for frustrated sc lattice at $x=0.45$. Lines are guides to the eye. Inset shows collapse of the data according to Eq. (19) using the exponent $\nu=0.704$. Where error bars are not apparent, they are smaller than the symbol size.

Finite size scaling theory predicts that in the vicinity of $T_{C,N}$, $m_{f,st}$ and $\chi_{f,st}$ scale according to

$$m_{f,st} = L^{-\beta/\nu} M(tL^{1/\nu}) \tag{20}$$

$$\chi_{f,st} = L^{\gamma/\nu} X(tL^{1/\nu}) \tag{21}$$

for large enough L. In Fig. 7, we show scaling plots for $m_{f,st}$ and $\chi^d_{f,st}$ at $x=0.45$, where it has been estimated[12] that $\beta/\nu \sim 0.35$ and, from hyperscaling, $\gamma/\nu=2.3$. In the four plots we have used the exponent ratios $\beta/\nu=0.514$ and $\gamma/\nu=1.973$, with $\nu=0.704$, as found for the pure Heisenberg model[26,27] ($x=0$) in three dimensions. The values of $T_{C,N}$ are taken from our Table II. The collapse is excellent for $8 \le L \le 24$, which strongly suggests that the transitions remain within the Heisenberg universality class.

Undoing the collapse of the x axis shown in Fig. 7 provides further support that the site-frustrated model remains in the Heisenberg universality class. If we plot $m_{f,st}L^{\beta/\nu}$ or $\chi^d_{f,st}L^{-\gamma/\nu}$ vs T for different L, then Eqs. (20) and (21) predict that we should observe a crossing of the data at $T_{C,N}$ similar to that observed for $B_{f,st}$, as shown in Fig. 6. In Fig. 8, we show such plots for the ferromagnetic transition at $x=0.45$—the same data used in the left panels of Fig. 7. A clear crossing is observed just below $T=0.95$.

We now turn to the form of the phase diagram near $x=0.5$. Aharony[4] first postulated the existence of a tetracritical point where the lines of second-order phase transitions, $T_C(x)$ and $T_N(x)$ cross. The phase diagram of Nielsen *et al.*[10] also exhibits a tetracritical point, as does the phase diagram of Matsubara *et al.*,[11] although in the latter case it was assumed. In contrast, it has been suggested[12] that the tetracritical point

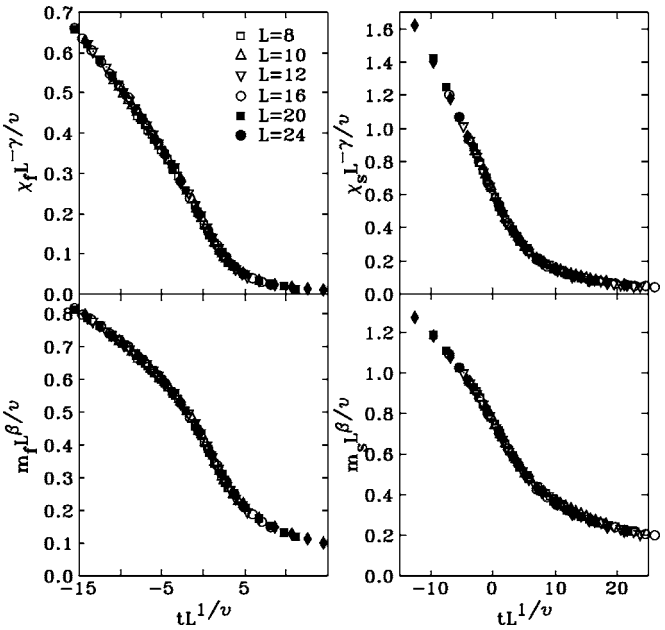

FIG. 7. Finite size scaling collapse of m_f and χ^d_f with $T_C=0.9491$ and m_{st} and χ^d_{st} with $T_N=0.6576$ for $L=8,10,12,16,20$, and 24. We have used the ratios $\beta/\nu=0.514$ and $\gamma/\nu=1.973$ of the three-dimensional Heisenberg universality class.

does not exist and instead there exists a regime from $0.48 < x < 0.52$ where $T_C(x)=T_N(x)$. We have recently reported[13] that the scaling of $T_{C,N}(L)$ according to Eq. (18) at $x=0.49, 0.495$, and 0.5 (for $L \le 20$ and $C=100$) disagrees with this conjecture. Our updated results at $x=0.49$ and $x=0.5$ (with $L \le 24$ and $C>200$), as listed in Table II, confirms that $T_C(x) \neq T_N(x)$ with the exception of $x=0.5$.

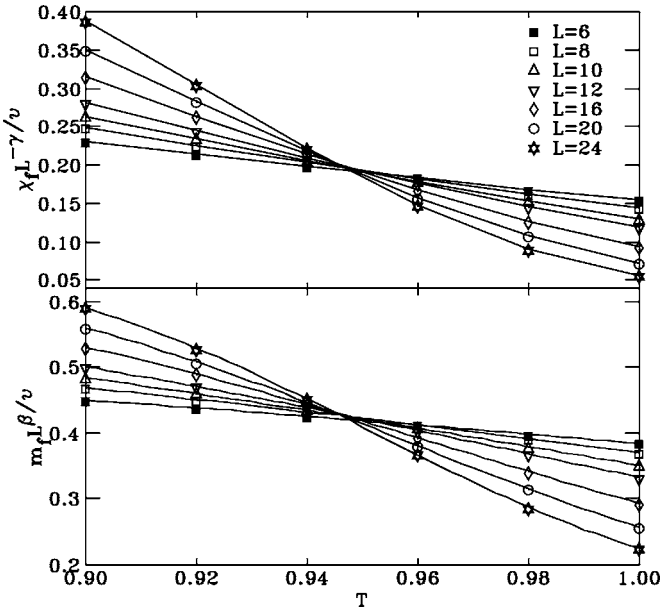

FIG. 8. Scaling plot of $m_f L^{\beta/\nu}$ and $\chi^d_f L^{-\gamma/\nu}$ vs temperature at $x=0.45$. Exponents are the same as in Fig. 7. A clear crossing is observed near $T_C=0.9491$. A further scaling the x axis according to $tL^{1/\nu}$ results in the collapse shown in Fig. 7. Where error bars are not apparent, they are smaller than the symbol size.

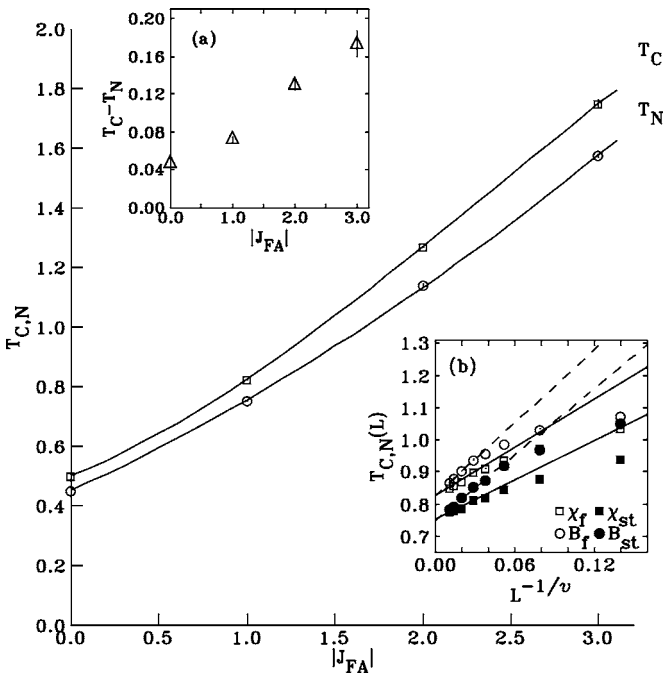

FIG. 9. T_C and T_N vs. $|J_{FA}|$ with $J_{FF}=-J_{AA}=+1$ for the sc lattice at $x=0.49$. Inset (a) shows the difference, T_C-T_N. Inset (b) shows the scaling of the pseudotransition temperatures for $J_{FA}=-1$. Where error bars are not apparent, they are smaller than the symbol size.

Further evidence in favor of a tetracritical point is provided by examining the behavior of the transition temperatures while varying the magnitude of the intersite coupling $|J_{FA}|$. Setting $J_{FA}=0$ decouples F and A sites, giving the nonfrustrated model and, hence, $T_C=T_N$ *only* at $x=0.5$. Elsewhere, $T_C \neq T_N$ and the phase diagram possess a decoupled tetracritical point at $x=0.5$. If the ordering scenerio in Ref. 12 were correct and $T_C=T_N$ at $x=0.49$ when $J_{FA}=1$, then T_C and T_N would evolve with increasing J_{FA} such that the two transition temperatures merged. Conversely, if the transition temperatures remain distinct, as one expects if the site-frustrated model possess a tetracritical point, then T_C and T_N must remain distinct as J_{FA} increases.

In Fig. 9, we show the evolution of both T_C and T_N at $x=0.49$ for the sc lattice with $J_{FA}=0$, -1, -2, and -3. It is clear from the plot that both T_C and T_N increase with increasing J_{FA} in this regime, and that T_C is never equal to T_N. In Fig. 9(a), we show the difference, T_C-T_N, which clearly indicates that the transition temperatures do not merge. Instead, the difference steadily increases (the difference between T_C and T_N is $>10\sigma$). We have observed[28] the same behavior for the bcc lattice at $x=0.4$ up to $J_{FA}=30$. As shown in Fig. 9(b), the scaling of the pseudotransition temperatures (as in Fig. 5) at $x=0.49$ with $J_{FA}=-1$ is typical of all our measurements and does not indicate anything that might suggest that $T_C=T_N$. We conclude that the site-frustrated model possess a tetracritical point at $x=0.5$ and that $T_C \neq T_N$ for all other x.

IV. DISCUSSION

A. Frustration density and distribution

To understand the phase diagrams of the site-frustrated Heisenberg model, it is necessary to consider both the density and distribution of frustration within the model. The density of frustration can easily be calculated from the probability that a plaquette exists in a frustrated configuration. In Fig. 10, we show examples of frustrated plaquettes for a four-spin plaquette, appropriate for sc and bcc lattices, and for a three-spin plaquette, appropriate for fcc lattices. In the case of sc and bcc lattices, site-frustrated models produce frustrated plaquettes *only* when the plaquette contains two neighboring F sites and two neighboring A sites. For fcc lattices, a plaquette is frustrated when it contains either two or three A sites. The density of frustrated plaquettes x_f is

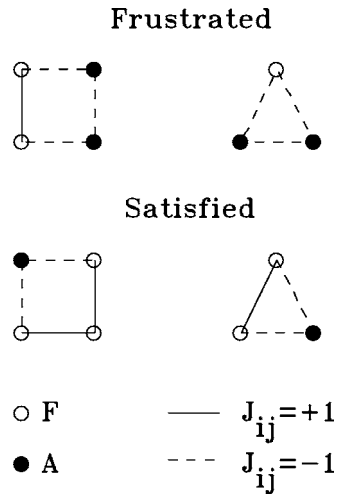

FIG. 10. Examples of frustrated and satisfied plaquettes for the site-frustrated model for a four-spin plaquette geometry appropriate for sc and bcc lattices and for a three-spin plaquette geometry appropriate for fcc lattices.

$$x_f = 4x^2(1-x)^2 \tag{22}$$

for sc and bcc lattices and

$$x_f = 3x^2(1-x) + x^3 \tag{23}$$

for fcc lattices. In the same way, the density of frustrated plaquette in the *bond*-frustrated model is

$$x_f = 4x(1-x)^3 + 4x^3(1-x) \tag{24}$$

for sc and bcc lattices and

$$x_f = 3x(1-x)^2 + x^3 \tag{25}$$

for fcc lattices, where for bond-frustrated models x is the concentration of antiferromagnetic bonds, while for site-frustrated models x is the concentration of antiferromagnetic sites. The densities of frustrated plaquettes given by Eqs. (22)–(25) are plotted in Fig. 11.

If site and bond-frustrated models were gauge equivalent, as has been previously assumed,[5] then x_f would be the same for both the site-frustrated model and its gauge equivalent bond-frustrated counterpart, since x_f is gauge invariant. The site-frustrated model on sc and bcc lattices has a maximum of $x_f=0.25$, and thus, the assumed gauge equivalent bond-frustrated model must have $x<0.08$ (or $x>0.92$), so that $x_f \leq 0.25$ (see Fig. 11). At this concentration of antiferromagnetic (ferromagnetic) bonds, $3d$ bond-frustrated models are

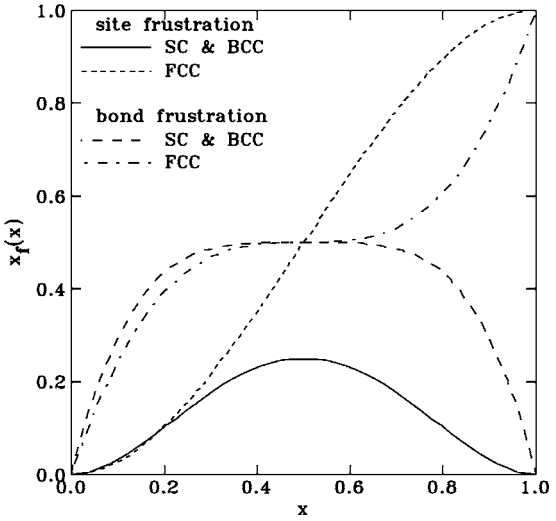

FIG. 11. The density of frustration for site- and bond-frustrated models on sc, bcc, and fcc lattices. Note that the density of frustration is much less for the site-frustrated model on sc and bcc lattices as compared to the bond-frustrated model.

ordered ferromagnets[24,29,30] (antiferromagnets). Assuming gauge equivalence between site- and bond-frustrated models in three dimensions shows that the site-frustrated model consists[31] of FM or AF order for all x, and rules out the possibility of spin-glass order. This result is in direct contradiction of the assumption[5] that the equivalence of bond and site frustration leads to spin-glass order in site-frustrated models.

It is easy, however, to prove that site and bond frustration are *not* gauge equivalent on bipartite lattices. To do so, consider the probability that, given a frustrated plaquette, all of the neighboring plaquettes exist in a frustrated configuration. For a bond-frustrated model, this probability is finite for $0 < x < 1$, whereas for site-frustrated models this probability is zero for $0 \leq x \leq 1$, which is sufficient to prove that site- and bond-frustrated models are not gauge equivalent.

It is also interesting to note that the site-frustrated model on an fcc lattice exists as an ordered ferromagnet until $x_f \sim 0.9$ ($x \sim 0.8$) while for the sc *bond*-frustrated model ferromagnetism is lost by $x_f \sim 0.44$ [$x = 0.208(2)$] for Heisenberg[24] spins. This serves to emphasize that the density of frustration alone is not responsible for the destruction of periodic order, but the distribution, which, as we have shown, is quite different for site- and bond-frustrated models.

For sc and bcc lattices, frustrated plaquettes exist only when a plaquette contains two neighboring F sites and two neighboring A sites. If the lattice is considered to be a collection of F and A clusters, it follows that all of the frustrated plaquettes exist on the surfaces separating the clusters. Since all of the frustration exists at the interface, which separates clusters of F and A sites, unsatisfied bonds are likely to also reside near that interface. Given this situation, the phase diagrams of site frustrated models (Fig. 2) can be expected to mimic those of the nonfrustrated models (Fig. 3), as we have observed.

The effect of concentrating all of the frustrated plaquettes onto the surfaces separating clusters of F/A sites will be explored by considering simple Ising spins since algorithms exist for determining exact ground states. In two dimensions, ground states for Ising spins with $\pm J$ interactions are determined by pairing frustrated plaquettes with a line called a dual string. Bonds traversed by the dual string are broken with the remaining bonds satisfied. It then follows that the ground state is determined by minimizing the total length of all dual strings.[20]

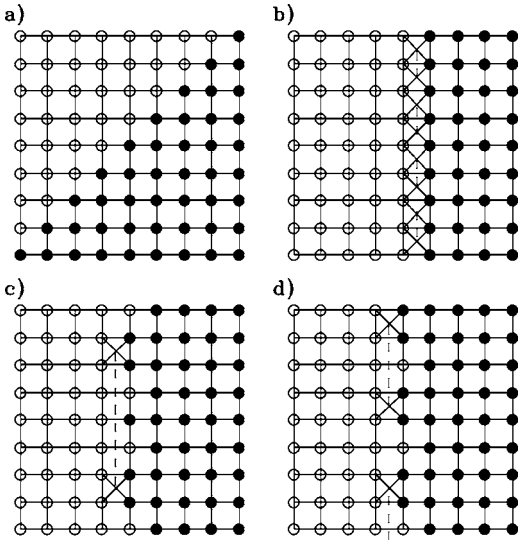

FIG. 12. Two-dimensional square lattices showing various possible interfaces between F and A sites where frustration occurs. (a) Flat (1 1) interface, no frustration. (b) Flat (1 0) interface, infinite number of frustrated plaquettes (crosses) on interface. (c) Two frustrated plaquettes separated by a finite distance, energy is proportional to the length of the dual string (broken line) linking them. (d) Rough (1 0) interface, random linear distribution of frustration. Only one of the two shortest linkings is shown.

We first consider a diagonal, (1 1), surface separating clusters of F and A sites. This configuration of bonds, shown in Fig. 12(a), has no frustration, and the ordering which takes place belongs to the pure, ferromagnetic, two-dimensional Ising universality class.

A (1 0) interface, shown in Fig. 12(b), while superficially similar to (1 1) interface, actually creates a configuration with an infinite number of frustrated plaquettes. The lowest energy state then consists of all F sites ordered ferromagnetically and all A sites ordered antiferromagnetically. Satisfied and unsatisfied bonds alternate along the interface leading to a two fold degeneracy, decoupling the two regions. The orientation of the FM order is free to point up or down with respect to a fixed AF order, this effectively mimics the model where $J_{FA} = 0$.

The third configuration we consider is two frustrated plaquettes separated by a finite distance shown in Fig. 12(c). The lowest energy state consists of F sites ordered FM and A sites ordered AF with a line of unsatisfied bonds along the shortest path connecting the two frustrated plaquettes. In this case, a preferred relative orientation (unidirectional anisotropy) is imposed on, for instance, the FM order if the AF ordering has already taken place.

The last configuration we consider consists of an interface with randomly placed frustrated plaquettes, shown in Fig.

12(d). The two shortest ways of connecting these plaquettes with dual strings (A–B, C–D, E–F, *etc.*, and B–C, D–E, F–G, *etc.*) need not have the same energy, leading to unidirectional anisotropy. However, for a very long interface, the difference in energy associated with these two possible linkings becomes infinitesimally small, and the FM-ordered F sites and AF-ordered A sites are again decoupled, mimicking the model with $J_{FA}=0$.

The examples considered here demonstrate that frustration at the interface of F/A clusters tends to either decouple the FM and AF ordering, Figs. 12(b) and 12(d), or to introduce unidirectional anisotropies, Figs. 12(c) and 12(d). This behavior will only occur if the dual strings, which link frustrated, plaquettes, reside near the interface and do not pass through the volume of the cluster. However, if we constrain our interest to percolating F/A clusters, the density of frustration at the interface is large ($\sim 25\%$) so that the total length of the associated dual strings linking the frustrated plaquettes will be minimized by using short elements traversing the interface. Equivalently, bonds that compose the volume of a percolating cluster, $\propto L^d$, are satisfied at the expense of the bonds at the interface of the percolating cluster, $\propto L^{d-1}$ leading to the conclusion that percolating clusters of F or A sites order FM or AF, identical to the respective pure models. Decoupling of the FM- and AF-ordered clusters will then occur when the number of satisfied and unsatisfied bonds at the interface are equal so that the ordered clusters are free to take any possible orientation.

Given the configuration of bonds in Fig. 12(b), where for Ising spins there is a decoupling of the AF and FM order, it can be imagined that for Heisenberg spins the energy of the system can be further reduced: If the AF and FM ordering directions are chosen to be mutually perpendicular, there is a net reduction in the interface energy if the AF-ordered spins near the interface cant either up ($J_{FA}=+1$) or down ($J_{FA}=-1$) with respect to the FM order, minimizing exchange energy from the J_{FA} bonds at the expense of the J_{AA} bonds. This net energy change would then give rise to mutually perpendicular FM and AF order.[11] The perpendicular nature of the FM and AF order is shown in Fig. 13, where we depict the parallel and perpendicular components of m_{st} with respect to m_f for both the frustrated and nonfrustrated models.[32] The situation is analogous to isotropic antiferromagnets in a uniform external field[33] where the AF ordering is transverse to the applied field, with the moments canting upward along the applied field in order to minimize the total energy.

The difference in phase diagrams between sc and bcc lattices compared to fcc lattices leaves open the possibility that spin-glass ordering is permissible for fcc lattices in the concentration regime $0.8<x<1$. However, we do not believe that spin-glass ordering occurs for fcc lattices. Rather, based on the observed phase diagrams for sc and bcc lattices, the percolating structure of A sites likely decouples and orders identically to the appropriate pure model: the geometrically frustrated fcc antiferromagnet. Ordering of the fcc Heisenberg antiferromagnet ($x=1$) occurs at $T=0.223$,[25] and thus, our phase diagram for fcc lattices lacks a line of low-temperature transitions $T_N(x)$ from $0.2<x\leq 1$, as we have not attempted to measure it. The FM ordering for fcc lattices,

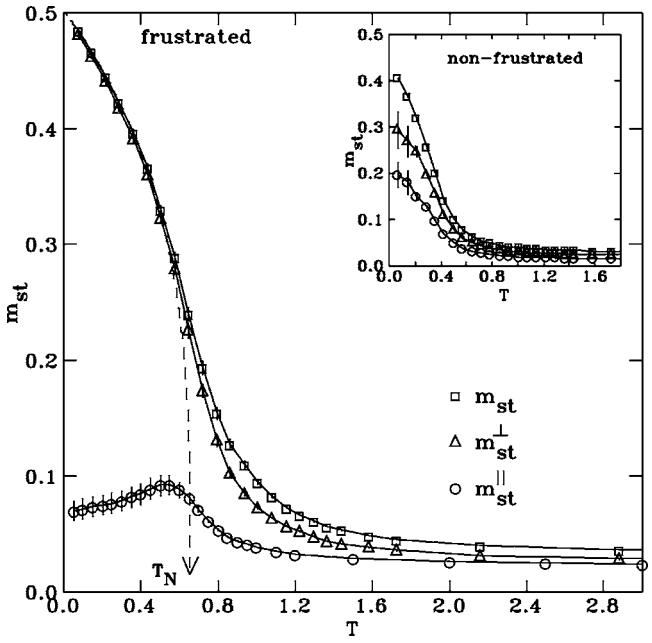

FIG. 13. Parallel ($m_{st}^{\parallel}$) and perpendicular ($m_{st}^{\perp}$) components of the total staggered magnetization (m_{st}) relative to the magnetization (m_f) for the site-frustrated Heisenberg model with $x=0.45$ for a sc lattice with $L=10$. The total staggered magnetization is also shown. Inset shows the same data for the nonfrustrated model ($J_{FA}=0$). It is evident that the effect of the J_{FA} bonds is to orient the AF order transverse to the FM order in the mixed phase.

which survives for an extremely high level of frustration $x_f \sim 0.9$ (almost twice that of the sc bond-frustrated model, which is a spin glass[34]) demonstrates again that it is not the amount of frustration that determines spin-glass order but its distribution. When frustration is pushed out to the surface of a percolating cluster, periodic ordering takes place.

B. Experimental consequences

The primary motivation for this work has been our experimental study of the amorphous alloy a-$(Fe_{1-x}Mn_x)$G.[2,3] In this alloy, Fe moments couple to neighboring Fe moments ferromagnetically and Mn moments couple to both Fe and Mn antiferromagnetically, hence, our choice $J_{FA}=-1$. The magnetic response of this alloy, therefore, may be considered prototypical of a site-frustrated magnet. An important difference between the model and the alloy is the disorder inherent to the glass structure. Despite this difference, many important details of the a-$(Fe_{1-x}Mn_x)$G phase diagram can be understood based on the model discussed here. For small x, the material remains ferromagnetic and the small concentration of Mn moments order antiparallel to the Fe-dominated FM order. Beyond a concentration of Mn sites $x\sim 0.2$, spin-glass-like ordering transverse to the magnetization occurs, which is dominated by Mn moments. This concentration corresponds to site percolation of Mn moments for an amorphous alloy[35] with 12 nearest neighbors. Because of structural disorder, the percolating cluster of Mn moments cannot order as a periodic AF and orders as a spin glass. The phase diagram of this alloy is likely to be captured by the fcc phase

diagram [Fig. 2(c)], where, in addition to FM ordering at T_C, a line of AF-type ordering characteristic of the fully frustrated Heisenberg antiferromagnet may occur at low temperatures. This transition, observed for the pure model[25] at $T_N=0.223$, is analogous to the spin-glass ordering occurring at T_{xy} for $x>0.2$ in a-$(Fe_{1-x}Mn_x)$G.

The transverse nature of the FM and AF order appears to be the only significant consequence of coupling the two types of sites together via J_{FA}. The FM and AF ordering is in no way weakened or destroyed by the frustrated coupling between the two types of sites. This result stands in stark contrast to claims that the ordering behavior of iron-rich a-Fe_xZr_{100-x} alloys is due to competition between antiferromagnetic clusters embedded in a ferromagnetic matrix,[36] and that ordering of the AF clusters destroys the preexisting FM order. Although there is now strong experimental evidence against this view,[37] the model studied here actually has this specific structure. For appropriate compositions, it could be described as a FM matrix with AF clusters, but the ordering of these AF clusters clearly does not destroy the preexisting FM order.

V. CONCLUSIONS

We have used Monte Carlo methods to investigate the ordering of Heisenberg spins on sc, bcc, and fcc lattices for a site-frustrated model. At all concentrations, the system forms at least one percolating network of F or A sites and, in the mixed phase, both F and A sites percolate. When both F and A sites percolate on bipartite lattices, they both order as one would expect if the frustration were removed, a fact readily apparent from the similarity between Figs. 2 and 3. In the case of the fcc lattice, AF ordering of A sites likely occurs for $0.2<x<1$, and thus, we expect that a tetracritical point should occur here as well. The resulting phase diagrams for frustrated (Fig. 2) and nonfrustrated models (Fig. 3) are closely related, sharing similar, if not the same, critical concentrations. The universality class of the transitions remain in the three-dimensional Heisenberg universality class, in agreement with the Haris criteria. The J_{FA} bonds coupling the A and F sites lead only to minor changes in the ordering: (i) The transition temperatures are slightly increased (see Fig. 9), and (ii) the F and A clusters have mutually perpendicular ordering directions (see Fig. 13).

For bipartite lattices, there is a tetracritical point at $x=\frac{1}{2}$ where FM and AF order develop simultaneously in the infinite percolating F and A clusters. The presence of long-range periodic order at all concentrations allows us to rule out spin-glass ordering in these models for bipartite lattices. In the case of fcc lattices, we have attempted to detect the ferromagnetic transition only. However, by analogy with the sc and bcc lattices, we expect that the percolating A cluster undergoes the ordering characteristic of the fully frustrated fcc model.

ACKNOWLEDGMENTS

This work was supported by grants from the Natural Sciences and Engineering Research Council of Canada, and Fonds pour la formation de chercheurs et l'aide à la recherche, Québec. We would also like to thank Juan Gallego for help with the Shire beowulf cluster.[38]

[1] D. H. Ryan in *Recent Progress in Random Magnets*, edited by D. H. Ryan (World Scientific, Singapore, 1992), p. 1.
[2] D. H. Ryan, A. D. Beath, E. McCalla, J. van Lierop, and J. M. Cadogan, Phys. Rev. B **67**, 104404 (2003).
[3] A. Kuprin, D. Wiarda, and D. H. Ryan, Phys. Rev. B **61**, 1267 (2000).
[4] A. Aharony, Phys. Rev. Lett. **34**, 590 (1975).
[5] S. Fishman and A. Aharony, Phys. Rev. B **19**, 3776 (1979).
[6] The site frustrated model of Ref. 5 was considered to be identical to a bond frustrated model, apart from short-range correlations which were considered unimportant in determining the long-range order.
[7] S. F. Edwards and P. W. Anderson, J. Phys. F: Met. Phys. **5**, 965 (1975).
[8] M. Gabay and G. Toulouse, Phys. Rev. Lett. **47**, 201 (1981).
[9] D. H. Ryan, J. van Lierop, M. E. Pumarol, M. Roseman, and J. M. Cadogan, J. Appl. Phys. **89**, 7039 (2001).
[10] M. Nielsen, D. H. Ryan, H. Guo, and M. Zuckermann, Phys. Rev. B **53**, 343 (1996).
[11] F. Matsubara, T. Tamiya, and T. Shirakura, Phys. Rev. Lett. **77**, 378 (1996).
[12] S. Bekhechi and B. W. Southern, Phys. Rev. B **70**, 020405(R) (2004).
[13] A. D. Beath and D. H. Ryan, J. Appl. Phys. **97**, 10A511 (2005).
[14] A. B. Harris, J. Phys. C **7**, 1671 (1974).
[15] R. B. Stinchcombe in *Phase Transitions and Critical Phenomenon* edited by C. Domb and M. S. Green (Academic Press, New York, 1983), Vol 7.
[16] D. Stauffer, *Introduction to Percolation Theory* (Taylor & Francis, London, 1985).
[17] D. C. Mattis, Phys. Lett. **56A**, 421 (1976).
[18] J. M. Luttinger, Phys. Rev. Lett. **37**, 778 (1976).
[19] G. Toulouse, Commun. Phys. (London) **2**, 115 (1977).
[20] E. Fradkin, B. A. Huberman, and S. H. Shenker, Phys. Rev. B **18**, 4789 (1978).
[21] H. Muller-Krumbharr and K. Binder, J. Stat. Phys. **8**, 1 (1973).
[22] R. G. Brown and M. Ciftan, Phys. Rev. B **54**, 15860 (1996).
[23] M. Creutz, Phys. Rev. D **36**, 515 (1987).
[24] A. D. Beath and D. H. Ryan, J. Appl. Phys. **97**, 10A506 (2005).
[25] J. L. Alonso, A. Tarancón, H. G. Ballesteros, L. A. Fernández, V. Martín-Mayor, and A. Muñoz Sudupe, Phys. Rev. B **53**, 2537 (1996).
[26] C. Holm and W. Janke, Phys. Rev. B **48**, 936 (1993).
[27] K. Chen, A. M. Ferrenberg, and D. P. Landau, Phys. Rev. B **48**, 3249 (1993).
[28] A. D. Beath and D. H. Ryan, J. Appl. Phys. **95**, 6980 (2004).
[29] A. Ghazali, P. Lallemand, and H. T. Diep, Physica A **134**, 628 (1986).

[30] J. R. Thomson, H. Guo, D. H. Ryan, M. J. Zuckermann, and M. Grant, Phys. Rev. B **45**, 3129 (1992).

[31] The FM/AF order in the equivalent site frustrated model may be hidden, in the sense that the FM order in Mattis models is hidden. However, since bond frustrated models remain in the Heisenberg universality class for $x < 0.2$, the hidden order would also be within the Heisenberg universality class.

[32] The data shown in Fig. 13 are obtained using Metroplolis dynamics. To observe the correct behavior, we must exceed τ for the *vector* quantities such that $\vec{m}_f$ and $\vec{m}_{st}$ complete many orbits. In addition, these long runs (using $\sim 5 \times 10^6$ MCSs at low temperatures) provide a good check for convergence of the scalar quantities (where, typically, we use $\sim 5 \times 10^4$ OR-MCSs).

[33] L. Neél, Ann. Phys. (Paris) **18**, 5 (1932).

[34] L. W. Lee and A. P. Young, Phys. Rev. Lett. **90**, 227203 (2003).

[35] M. Ahmadzadeh and A. W. Simpson, Phys. Rev. B **25**, 4633 (1982).

[36] S. N. Kaul, J. Phys.: Condens. Matter **3**, 4027 (1991).

[37] D. H. Ryan, J. M. Cadogan, and J. van Leirop, Phys. Rev. B **61**, 6816 (2000).

[38] Information on our computer cluster, named the shire, can be found at www.physics.mcgill.ca/~juan/shire/